Short communication

Dissolution of coated microbubbles: The effect of nanoparticles and surfactant concentration

M. Azmin, G. Mohamedi, M. Edirisinghe, E.P. Stride *

Mechanical Engineering Department, University College London, Torrington Place, London, WC1E 7JE, UK

ABSTRACT

The ability of solid particles to stabilise emulsions is a well known phenomenon which has recently been demonstrated for the stabilisation of gas bubbles. In this paper, a new theoretical model is developed which describes how an adsorbed layer of solid nanoparticles modifies the interfacial tension and diffusivity of a gas bubble in a liquid and hence its stability. In agreement with experimental observations on micro-bubbles coated with 15 nm diameter spherical gold particles, the results of simulations with the model indicate that the particles substantially decrease the rate at which bubble dissolution occurs and enables them to maintain a stable radius once a critical particle concentration has been reached.

© 2012 Elsevier B.V. All rights reserved.

1. Introduction

Gas microbubbles are of considerable interest in a range of both diagnostic and therapeutic medical applications including contrast enhancement in ultrasound imaging [1], targeted drug delivery and gene therapy [2]. Since they are normally used as vascular agents, the bubbles cannot be more than a few micrometres in diameter to avoid the risk of causing an embolism. A bubble smaller than ~100 μm in diameter, however, will rapidly dissolve when placed in a liquid, due to interfacial tension and the gas concentration gradient across the bubble surface. In order to counter this instability, micro-bubbles used as imaging or therapeutic agents are coated, most commonly with surface active molecules which self assemble at the liquid/gas interface in an aqueous liquid environment. This adsorption results in a reduction of both the interfacial tension and the diffusivity of the gas across the bubble surface [3].

Previously, it was reported that surface deposition of nanoparticles on microbubbles can enhance the nonlinearity of their oscillations [4]. This is a desirable property for ultrasound contrast enhancement and for therapeutic monitoring as it improves detectability. In this study it was also observed that this deposition of particles greatly enhances the stability of the microbubbles. Fig. 1 shows micrographs of air bubbles prepared using a microfluidic device coated with a surfactant (PEG-40-stearate) and an aqueous suspension of spherical gold nanoparticles (15 nm mean diameter) that undergo a negligible change

in size over 3 days compared with bubbles coated with the same surfactant but no particles which disappeared within 24 h. Experimental details relating to bubble preparation may be found in Stride et al. [4].

The ability of small particles to stabilise colloid dispersions of larger particles was first described by Ramsden [5] and later by Pickering [6] and there are many examples in the literature where this method has been used to increase the stability of an emulsion [7]. The aim of this study was to derive a theoretical model to describe the effect upon the stability of a gas microbubble of the adsorption of nanoparticles on to its surface.

2. Theory

Fick's 1st law states that the rate of mass transfer (flux) per unit area, J, of a component of concentration C across a plane is proportional to the concentration gradient across that plane. This is expressed in spherical polar coordinates as:
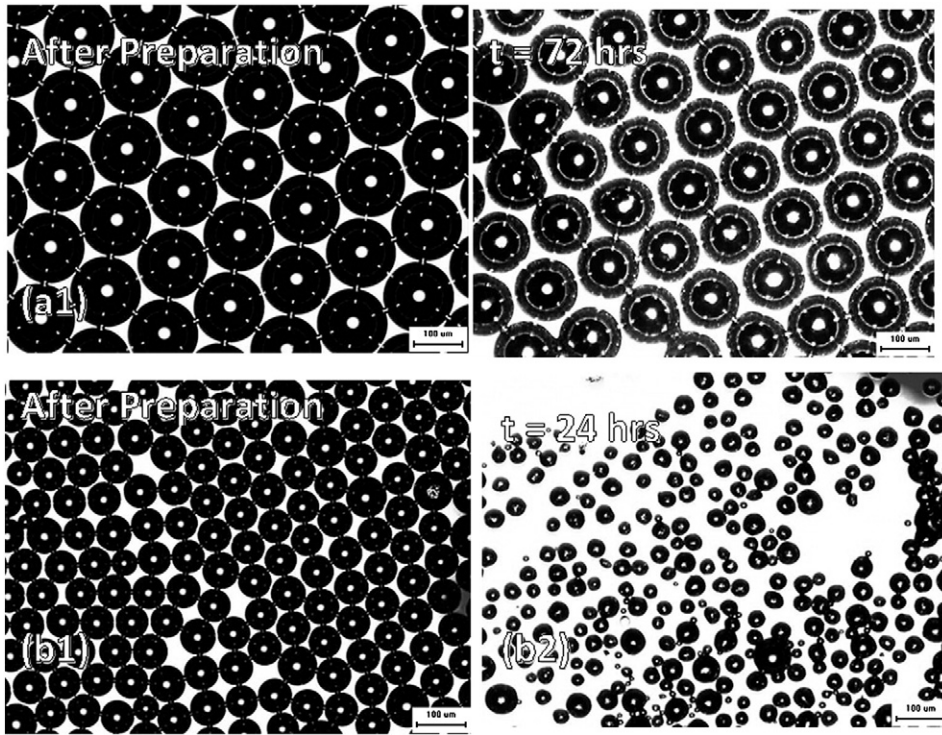
$$J = -D\frac{\partial C}{\partial r} \tag{1}$$

where D is the diffusivity of the component in the surroundings and r is the distance measured from the origin. For the case of a spherical gas bubble (Fig. 2) of radius $R(t)$ centred at $r = 0$ in a liquid of infinite volume Epstein and Plesset [8] derive an equation for $\left(\frac{\partial C}{\partial r}\right)_R$ as:

$$\left(\frac{\partial C}{\partial r}\right)_R = (C_i - C_{sat}(R))\left[\frac{1}{R} + \frac{1}{(\pi D t)^{\frac{1}{2}}}\right] \tag{2}$$

Fig. 1. Comparison of the stability of two microbubble suspensions prepared in a microfluidic T-junction device: a) microbubbles coated with gold nanoparticles and a surfactant (PEG-40 stearate); b) microbubbles coated with surfactant only. It can be clearly observed that the microbubble population with the nanoparticle coating has undergone a 15% reduction in mean diameter with the sample remaining relatively monodisperse after 72 h. The microbubble sample without the nanoparticle coating has undergone a much larger (average 50%) reduction in size and change in size distribution after only 24 h. It may be noted that the microbubbles in a1 are larger and more uniform than those shown in b. This is because, although the two suspensions were prepared in an identical fashion and initially has the same mean size, over the short time required to transfer the samples to the microscope the bubbles coated only with surfactant had started to undergo change in size.

where C_i and $C_{sat}(R)$ are the initial concentration of the gas in the liquid and the dissolved gas saturation concentration at the bubble wall respectively. It is assumed that C_i, the temperature (T) and pressure (p) are constant throughout the liquid and that Henry's law

Fig. 2. Schematic of a microbubble with surfactant and nanoparticle coating suspended in an infinite liquid of variable dissolved gas content. The thickness of the shell is in reality much smaller than the bubble radius but has been exaggerated here for illustration purposes.

applies at the gas/liquid interface. The mass flow rate through the boundary can then be written as:

$$\frac{dm}{dt} = S_A D \left(\frac{\partial C}{\partial R}\right)_R = 4\pi R^2 D(C_i - C_{sat}(R)) \left[\frac{1}{R} + \frac{1}{(\pi D T)^{\frac{1}{2}}}\right] \qquad (3)$$
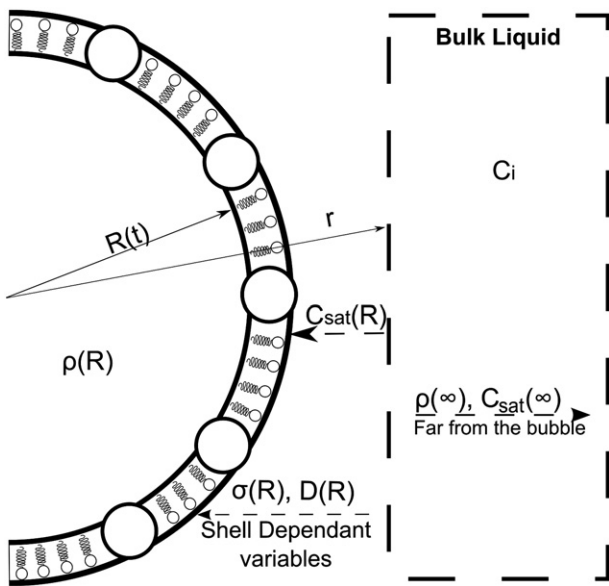
where S_A is the instantaneous surface area of the bubble. In order to find an equation for the rate of change of bubble radius, Eq. (3) can be incorporated in an equation describing the rate of change of the mass of a bubble, m, under constant interfacial tension, σ:

$$\frac{dm}{dt} = 4\pi R^2 \left(\frac{dR}{dt}\right)\left[\rho(\infty) + \frac{4M\sigma}{3BTR}\right] \qquad (4)$$

where B is the universal gas constant, M is the molecular weight of the gas, ρ is the density of the gas in the bubble and the term (∞) denotes conditions in the bulk liquid (i.e. neglecting the additional pressure on the gas due to surface tension). Equating Eq. (4) with Eq. (3) gives:

$$\frac{dR}{dt} = \frac{D(C_i - C_{sat}(R))}{\rho(\infty) + \frac{2M}{3BT}\frac{2\sigma}{R}} \left[\frac{1}{R} + \frac{1}{(\pi D t)^{\frac{1}{2}}}\right]. \qquad (5)$$

It should be noted that in deriving Eq. (5), convection has been neglected. The fully coupled mass transport problem was solved by Ready and Cooper [9] and Weinberg [10]. It was found that the effects of convection, particularly for bubbles with diameter of less than 1 mm, were however very small. The following derivation will therefore concentrate on the effects of surfactants and solid particles upon bubble dissolution.

The effect of a surfactant coating is to reduce the interfacial tension as well as providing a barrier to mass transfer across the bubble wall. These effects become increasingly significant with increasing surface concentration of surfactant molecules (Γ). For an insoluble molecular monolayer, the interfacial tension $\sigma(R)$ can be written as [11,12]:

$$\sigma(R) = \int -2\Gamma_0 \frac{\partial \sigma}{\partial \Gamma} \frac{R_0^2}{R^3} dR = \sigma_0 + \frac{K\Gamma_0^{x+1}}{x+1}\left(1 - \left(\frac{R_0}{R}\right)^{2(x+1)}\right) \quad (6)$$

where Γ_0 is the initial surfactant concentration on the bubble surface at which $\sigma = \sigma_0$, $R = R_0$, and K and x are constants characterising a given surfactant. Similarly, the coefficient of diffusion in the presence of a surfactant coating will also be a function of surface concentration, which in turn is a function of bubble radius. Using a similar treatment to that of Cable and Frade [13] $D(R)$ can be written as the exponential function:

$$D(R) = aD_0 \exp\left(b\left(1 - \left(\frac{R_0}{R}\right)^2\right)\right) \quad (7)$$

Again a, b and D_0 characterise a given surfactant. When nanoparticles are adsorbed on to the interface of a dissolving microbubble, they affect its dissolution in two ways. First, they reduce the effective surface area available for the diffusion of gas molecules through the interface. As the radius of the bubble decreases, the particles remain on the interface and therefore their fractional coverage of the surface area of the bubble increases. Thus the uncovered interfacial surface area can be written as:

$$S_A(R) = 4\pi R^2\left(1 - f_{P0}\left(\frac{R_0}{R}\right)^2\right) \quad (8)$$

where f_{p0} is the initial fractional coverage of particles on the bubble surface. The second stabilisation mechanism comes into effect as the bubble shrinks further. As the radius decreases, the particles on the interface become increasingly close to each other and the radius of curvature of the interface between them increases. There will come a point when the particles reach their packing density and the interface can become flattened (Fig. 3).

At this point the capillary or Laplace pressure, p_L, at the bubble surface due to interfacial tension will be reduced to zero since:

$$p_L = \frac{2\sigma}{r_c} \quad (9)$$

where r_c is the interfacial radius of curvature; as $r_c \to \infty$, $p_L \to 0$.

Following the derivation method of Epstein and Plesset but using the terms described in Eqs. (6), (7) and (8):

$$\frac{dR}{dt} = \frac{(C_i - C_{sat}(R))}{\rho(\infty) + \frac{2M}{3BT}\frac{2}{R}\left[\sigma_0 + \frac{K\Gamma_0^{x+1}}{x+1}\left[x\left(\frac{R_0}{R}\right)^{2(x+1)} + 1\right]\right]}\left[\frac{D(R)}{R} + \sqrt{\frac{D(R)}{\pi t}}\right]\left[1 - f_{p0}\left(\frac{R_0}{R}\right)^2\right] \quad (10)$$

It should be noted that for the case of a variable diffusivity, Eq. (2) now represents an approximation to the true boundary condition, but the additional terms in the series will be small (cf. Eq. (6) of Epstein and Plesset). As above, the dissolved gas content at the bubble wall is a function of pressure and will therefore also vary as the bubble internal pressure changes. Following Epstein and Plesset, the following relations can be defined:

$$f = \frac{C_i}{C_{sat}(\infty)}, \tau = \frac{2M}{BT} \text{ and } d = \frac{C_{sat}(\infty)}{\rho(\infty)} = \frac{C_{sat}(R)}{\rho(R)} = \frac{C_{sat}(R)}{\rho(\infty) + \frac{\tau\sigma(R)}{R}}.$$

Here f is the ratio of the initial gas concentration to the concentration at saturation in the bulk liquid and d is the ratio of saturated dissolved gas to gas density. It is assumed that the value of d is not affected by changes in surface tension again according to Epstein and Plesset. Using these relationships Eq. (10) now becomes:

$$\frac{dR}{dt} = d\frac{f - 1 - \frac{\tau\sigma(R)}{R\rho(\infty)}}{1 + \frac{2\tau}{3R\rho(\infty)}\left[\sigma_0 + \frac{K\Gamma_0^{x+1}}{x+1}\left[x\left(\frac{R_0}{R}\right)^{2(x+1)} + 1\right]\right]}\left[\frac{D(R)}{R} + \sqrt{\frac{D(R)}{\pi t}}\right]\left[1 - f_{p0}\left(\frac{R_0}{R}\right)^2\right]. \quad (11)$$

3. Results and discussion

Eq. (11) was non-dimensionalised in terms of the new variables: $x'^2 = 2dD_0t/R_0^2$ and $\varepsilon = R/R_0$ and solved numerically using a 4th order Runge–Kutta method (via function ODE45 in MATLAB, R2010b, MathWorks Inc.). Fig. 4 shows how the bubble radius changes with time with different initial concentrations of particles, f_{p0}, on the bubble surface in a gas saturated solution at constant temperature and pressure. As expected, for the particle coated bubbles, the rate at which the bubbles dissolve decreases with time due to the increasing proximity of the particles on the bubble surface. Since there is no gas concentration gradient between the bubble and the surrounding liquid in a gas saturated solution, the bubbles reach a stable size and the higher the initial particle concentration the more rapidly the bubble reaches this size and the larger it is.

Fig. 5 demonstrates the effect of reducing the dissolved gas concentration in the surrounding liquid so that $f = 0.75$. Once again the rate of bubble dissolution decreases with increasing initial surface concentration but now there is a finite gas concentration gradient across the bubble surface which remains even after the particles on the bubble surface have reached their maximum concentration. Since it is implicitly assumed in the above equations that the bubble
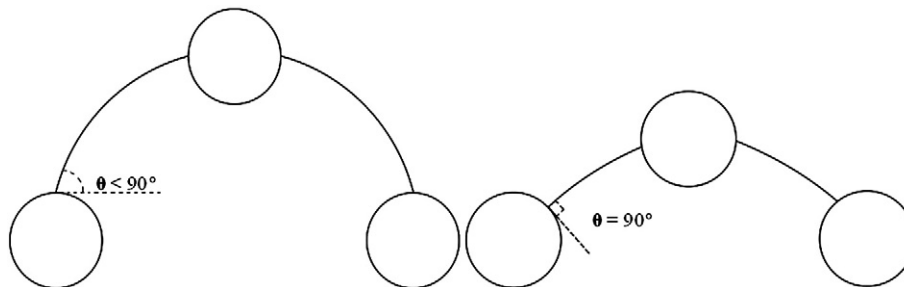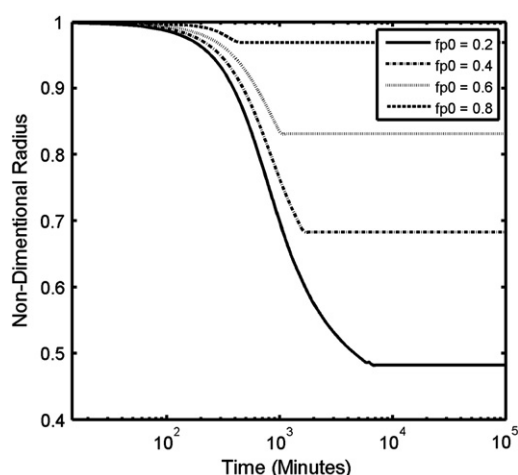

Fig. 3. Schematic of the effect of decreasing inter-particle spacing on the curvature of the bubble surface. As the particles become ever closer, the radius of curvature for the interface between them increases.

Fig. 4. Radius–time curve for a spherical air bubble in gas saturated liquid ($f = 1.00$) and various initial particle concentrations. The following parameters were used: $a = 0.5$, $b = 2$, $D_0 = 2.0 \times 10^{-9}$ m^2/s, $K = 1.5 \times 10^{-18}$, $\Gamma_0 = 1.0 \times 10^{14}$ molecules/m^2, $\sigma_0 = 0.062$ N/m, $\rho_\infty = 1.204$ kg/m^3.

remains spherical and that the particles are rigid, the radius of the bubble as would be observed experimentally cannot undergo further change. The amount of gas inside the bubble could, however, continue to decrease and this is illustrated in Fig. 5 which shows how the effective bubble volume would change due to ongoing gas diffusion. This process could continue until either: the curvature of the bubble surface between the particles becomes convex and the Laplace pressure becomes sufficiently negative that the direction of gas diffusion is reversed, or, the close packed particle structure buckles. These effects are not described by Eq. (10) and the long term behaviour of the bubbles must therefore be considered indeterminate. The assumption of sphericity, is in agreement with the authors' experimental observations (Fig. 1), but other studies with much larger particle to bubble diameter ratios have shown that non-spherical bubble shapes can also be stably maintained [14]. Similarly, the assumption that as the bubble shrinks the surface layer remains one-particle thick and none are ejected due to the stresses resulting from interfacial tension is supported by surface energy considerations and free energy analysis [15]; but it is possible that this is not retained over long periods.
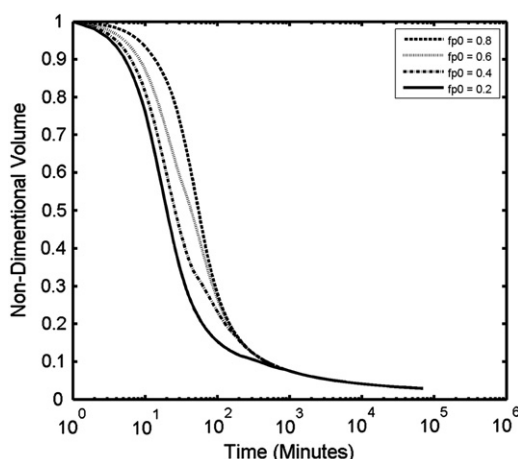
Fig. 5. Effective volume–time curve for a spherical bubble where $f = 0.75$ and for various initial particle concentrations. The following parameters were used: $a = 0.5$, $b = 2$, $D_0 = 2.0 \times 10^{-9}$ m^2/s, $K = 4.8 \times 10^{-18}$, $\Gamma_0 = 1.0 \times 10^{14}$ molecules/m^2, $\sigma_0 = 0.062$ N/m, $\rho_\infty = 1.204$ kg/m^3. The volume plotted is the effective volume that the bubble would have as a result of ongoing gas diffusion from the bubble into the liquid. The size of the bubble which would actually be observed experimentally however would not changed due to the particle jamming effect.

There are a number of additional assumptions made in deriving Eq. (10) which should be discussed. First, in obtaining the relation between bubble radius and surface concentration, the transport of surfactants into the bulk liquid has been ignored, making it valid only for insoluble surfactants. In fact it has been suggested that soluble surfactants have little effect on resistance to mass transfer through the bubble shell [16]. Second, the effective diffusion coefficient was modelled using a simple exponential function which has not been experimentally verified for the surfactants relevant for biomedical microbubble agents since there are unfortunately few surfactants for which the relationship between the resistance to mass transfer and interfacial concentration has been fully characterised. Furthermore, the effect of surface hardening [17], when the surfactant molecules reach a critical packing density and provide a mechanical resistance to counter Laplace pressure similar to the particle jamming effect, has not been incorporated into the model. It has also been assumed that the nanoparticles are rigid and will not deform. The bubble sizes considered here are larger than those which are relevant for medical applications. Eq. (10) is valid for smaller bubbles down to a few 100 nm, but particle stabilisation has yet to be experimentally demonstrated for bubbles in the 1–10 μm range. These will both be pursued in future work together with a direct quantitative comparison between theoretical and experimental results.[1]

A further important consideration in the case of biomedical agents is that they typically contain high molecular weight gases (e.g. perfluorocarbons) not naturally present in the body and these undergo substitution with dissolved gases in the blood following injection [18]. The model proposed here could, however, be modified to account for dissolution behaviour in a multi-gas environment. This would be achieved by writing the gas pressure inside the microbubble as the sum of the partial pressures of its various constituent species resulting in a new equation of state for each of the gases at the bubble boundary. Applying Henry's law would result in a concentration equation at the boundary and in the bulk liquid for each of the species which could then be used to re-derive new forms of Eqs. (3) and (4) and hence a new model consisting of a set of equations to describe the rate of change of bubble size.

4. Conclusions

A new theoretical model has been derived to describe the influence of interfacially adsorbed solid particles upon the dissolution of a gas bubble in a liquid. Numerical simulations indicate that both the interfacial tension and diffusivity at the bubble surface can be substantially reduced by the presence of particles to the extent the bubble can maintain a stable radius if the particle concentration is sufficiently high. This is in agreement with experimental observations. Further investigation and model development is required to fully characterise the behaviour of the bubble under low concentrations of dissolved gas in the surrounding liquid and in the presence of soluble surfactants.

---

[1] This unfortunately could not be performed with the existing experimental results as the current method of microbubble production results in a close packed population of monodisperse bubbles. Consequently, the assumption that the microbubble is in an infinite liquid with a spherically symmetric gas concentration gradient is invalidated. In addition, the effect of close packing of the microbubbles where there are no nanoparticles is eventual coalescence as the result of Ostwald ripening which cannot be captured by the model.

References

[1] D. Cosgrove, N. Lassau, Eur. J. Nucl. Med. Mol. Imaging 37 (2010) S65–S85.
[2] K. Ferrara, R. Pollard, M. Borden, Annu. Rev. Biomed. Eng. 9 (2007) 415–447.
[3] M. Borden, M. Longo, Langmuir 18 (2002) 9225–9233.
[4] E. Stride, K. Pancholi, M. Edirisinghe, S. Samarasinghe, J. R. Soc. Interface 5 (2008) 807–811.
[5] W. Ramsden, Proc. R. Soc. 72 (1903) 156–164.
[6] S. Pickering, J. Chem. Soc. Trans. 91 (1907) 2001–2021.
[7] Z. Du, M. Bilbao-Montoya, B. Binks, E. Dickinson, R. Ettelaie, B. Murray, Langmuir 19 (2003) 3106–3108.
[8] P. Epstein, M. Plesset, J. Chem. Phys. 18 (1950) 1505–1509.
[9] D. Readey, A. Cooper, Chem. Eng. Sci. 21 (1966) 917–922.
[10] M. Weinberg, Chem. Eng. Sci. 36 (1981) 137–141.
[11] J. Israelachvili, Intermolecular and Surface Forces, Third ed. Academic Press, 2011.
[12] E. Stride, Philos. Trans. R. Soc. A 366 (2008) 2103–2115.
[13] M. Cable, J. Frade, Chem. Eng. Sci. 42 (1987) 2525–2530.
[14] A. Subramaniam, M. Abkarian, L. Mahadevan, H. Stone, Nature 438 (2005) 930.
[15] S. Kam, W. Rossen, J. Colloid Interface Sci. 213 (1999) 329–339.
[16] J. Caskey, W. Barlage, J. Colloid Interface Sci. 41 (1972) 52–62.
[17] W. Wang, C. Moser, M. Wheatley, J. Phys. Chem. 100 (1996) 13815–13821.
[18] J. Kwan, M. Borden, Langmuir 26 (2010) 6542–6548.

Mohan Edirisinghe DSc. holds the Bonfield Chair of Biomaterials in the Department of Mechanical Engineering at UCL. He has published over 300 journal papers and his most recent research is on advanced jet techniques for the preparation of novel biostructures including microbubbles and drug delivery capsules. He has been awarded many prizes for his work including the 2012 UK Biomaterials Society President's prize.
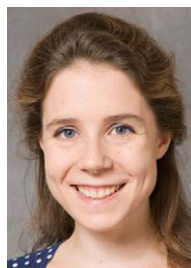
Eleanor Stride holds a BEng. and PhD from University College London. Following the completion of her PhD in 2005, she was appointed to a lectureship and a Royal Academy of Engineering and EPSRC Research Fellowship and subsequently a readership in 2010. She joined the Institute of Biomedical Engineering in Oxford in October 2011 where her key research interests are encapsulation, ultrasound therapy and medical imaging.

Mehrdad Azmin obtained his BEng and MSc in Mechanical Engineering at University College London. He has worked on the theoretical modelling of transient cavitation thresholds for both coated and uncoated bubbles and of the effects of rectified diffusion on stable cavitation. He is currently studying for his PhD on methods for modifying the stability and acoustic response of microbubble contrast agents for medical ultrasonic diagnosis and therapeutic applications.
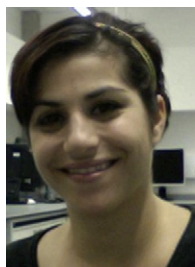
Grace Mohamedi graduated with a BSc in Chemical Engineering from the University of Rochester in 2008. She then worked as a research engineer at the University of Rochester Laboratory for Laser Energetics (LLE). During her time at the LLE she completed a combined research based MSc in Chemical Engineering and Optics, with a focus on Interfacial Engineering of optical materials as a result of which she received two international patents for novel capsule systems. In 2010 Grace began her work on engineering nanoparticle-loaded microbubbles for enhanced non-linear response at UCL and subsequently the University of Oxford.